Exceptionally High H_{c2} Values in Alloyed Bulk Samples of Nb₃Sn

Manish Mandal , Chiara Tarantini , *Senior Member, IEEE*, William L. Starch ,
Peter J. Lee , *Senior Member, IEEE*, and David C. Larbalestier , *Fellow, IEEE*

Abstract—Nb₃Sn is the original high-field superconductor but understanding its optimization in wire forms, which are always inhomogeneous, is compromised by a lack of basic understanding of its true property variations when it is alloyed with H_{c2} enhancing additions (e.g., Hf, Ta, Ti, Zr). Since improving the high-field performance of Nb₃Sn is important for many future applications in high energy physics, fusion, and medicine, we are studying bulk binary and alloyed samples fabricated by ball milling its constituent powders and reacting them in a Hot Isostatic Press at pressures up to 2000 bar and temperatures up to 1800 °C. Remarkably, we found that these bulk samples, reacted to produce the A15 phase at temperatures between 1200 and 1800 °C, show minority traces of H_{c2} (0 K), evaluated with a 99% criterion, that reach almost 40 T, more than 27% higher than the best value previously reported for Nb₃Sn. These results are both scientifically interesting but potentially of great practical importance if they can be exploited for improving the high-field properties of Nb₃Sn wires. One caution is that these samples do not have added Cu as wires do and that the high H_{c2} reactions were all done at well above 1000 °C.

Index Terms—Nb₃Sn, upper critical field, H_{c2}.

I. INTRODUCTION

NB₃SN is an important superconductor for high-field magnet applications, like particle accelerators, Nuclear Magnetic Resonance, and nuclear fusion machines. Improvement of the high-field performance for Nb₃Sn wires is necessary for the realization of the Future Circular Collider to be built at CERN [1], [2], [3], [4] and is a high priority for the U.S. Magnet Development Program [5]. The high-field superconducting performance can be enhanced by introducing artificial pinning centers [6], [7] and improving the upper critical field (H_{c2}).

Manish Mandal and David C. Larbalestier are with National High Magnetic Field Laboratory, Applied Superconductivity Center, Florida State University, Tallahassee, FL 32306 USA, and also with the FAMU-FSU College of Engineering, Tallahassee, FL 32310 USA (e-mail: mmandal@magnet.fsu.edu; larbalestier@asc.magnet.fsu.edu).

Chiara Tarantini, William L. Starch, and Peter J. Lee are with National High Magnetic Field Laboratory, Applied Superconductivity Center, Florida State University, Tallahassee, FL 32306 USA (e-mail: tarantini@asc.magnet.fsu.edu; starch@asc.magnet.fsu.edu; lee@asc.magnet.fsu.edu).

There is a rich history of enhancing H_{c2} by means of alloying Nb₃Sn with different doping elements [8], [9], [10], [11], [12], [13], [14], [15]. According to the Ginzburg-Landau-Abrikosov-Gorkov (GLAG) theory, $H_{c2} \sim \gamma \rho_n T_c$, where ρ_n is the residual resistivity of the normal state, γ is the electronic specific heat coefficient, and T_c is the critical temperature. The increase in H_{c2} by alloying is believed to be due to the increase in ρ_n [9], [10] created by disorder in A15. Bulk samples are easy to fabricate, and their high compositional homogeneity and relatively large dimensions compared to those found in wires make them useful for the study of the impact of alloying on A15 properties. For this reason, we are making binary and alloyed bulk Nb₃Sn samples, which will allow us to independently investigate the GLAG parameters, γ and ρ_n, and to understand how alloying affects A15 lattice disorder and perhaps how H_{c2} can be enhanced beyond present limits.

Because of unexpected results, in this work, we focused only on the fabrication and characterization of both binary and alloyed bulk Nb₃Sn samples made using a hot isostatic press (HIP) reaction to investigate the impact of doping (with and without Ta) on the upper critical field evaluated by transport measurement.

II. EXPERIMENTAL DETAILS

Bulk samples weighing about 15 g were fabricated using the HIP method. Powders used for binary sample preparation were: Nb (−325 mesh, 99.99% purity) and Sn (−325 mesh, 99.8%). For ternary samples, Hf (−325 mesh, 99.6%) was added as a doping element. For the quaternary sample, Nb4at%Ta alloy (−200 mesh) was used. The constituent powders were weighed inside a dedicated glove box filled with ultrahigh purity Argon gas (99.9999% purity) to avoid possible oxidation and were mixed for 1 hour using a high-energy ball mill. The resulting powder was placed inside a rubber tube and densified using a cold isostatic press (CIP) to form a hard pellet. To prevent any contamination, the hard pellet from the CIP was wrapped with Ta foil. The wrapped pellet was placed inside a one-end-closed Nb-tube. The tube was Ar flushed 4-5 times and finally evacuated to a pressure of 28 ± 2 mTorr. The tube's opposite end was crimped and finally sealed by welding. The encapsulated tube was CIPped, and then, a variety of heat treatments reaching temperatures as high as 1800 °C were performed inside the HIP. The pressure inside the HIP was kept at 2000 bars throughout

TABLE I
PROPERTIES, COMPOSITIONS, AND HTS OF NB₃SN BULK SAMPLES

	Nb25Sn-HT1	(Nb2Hf)25Sn-HT2	(Nb1Hf)25Sn-HT3	(Nb2Hf)25Sn-HT3	(Nb4Ta1Hf)25Sn-HT4
Heat treatment	650 °C/16h + 1600 °C/58h	650 °C/16h + 1600 °C/48h	1600 °C/60h	1600 °C/60h	650 °C/16h + 1200 °C/48h + 1800 °C/37h
$\mu_0 H_{c2,99}$ (0 K), [T]	34.6	39.2	38.2	33.1	36.8
$\mu_0 H_{c2,90}$ (0 K), [T]	30.8	33.6	32.6	29.8	31.1
$\mu_0 H_{c2,50}$ (0 K), [T]	28.4	30.7	30.0	27.2	29.1
$\mu_0 H_{Irr,10}$ (0 K), [T]	27.6	30.2	29.8	26.7	28.6
$\mu_0 H_{Irr,1}$ (0 K), [T]	25.3	30.0	29.3	26.5	28.2
ρ(20 K), [$\mu\Omega \cdot cm$]	28.9	56.1	43.9	68.7	32.7
$T_{c,99,fit}$, [K] [a]	17.83	17.95	17.67	15.96	17.81
$\mu_0 \left. \left\| \frac{dH_{c2,99}(0)}{dT} \right\| \right\|_{T_c}$, [T/K][a]	2.80	3.15	3.11	2.99	2.98
At. % Sn in A15, %	25.30	26.30	25.20	23.80-24.00	25.02
At. % Hf in A15, %	-	0.40-0.60	0.40-0.55	0.90-0.96	0.13-0.16
At. % Ta in A15, %	-	-	-	-	2.80

[a]$T_{c,99,fit}$ is obtained from the 2-16 T WHH fit of the $H_{c2,99}$ data and the $H_{c2,99}$ slope is back-calculated from the WHH fit (see text).

the heat treatment (HT). The list of samples fabricated, and their corresponding heat treatments are listed in Table I.

After the heat treatment, bulk samples of 2 cm in length and ∼1 cm in diameter were obtained. Microstructural and standardless-EDS microchemical analyses were performed using a ZEISS EVO 10 scanning electron microscope (SEM). The transport measurements were made in 9 T and 16 T Quantum Design (QD) physical property measurement system (PPMS) instruments, while their T_c transitions were evaluated by zero field cooling in a 5.5 T QD magnetic property measurement system (MPMS) SQUID magnetometer. To determine normal and superconducting properties, we performed transport measurements on rectangular bars. Thin round slices (1–2 mm) from each large sample were cut using diamond wire saw and further cut to remove the outer edges. The cut samples were then polished to obtain a rectangular shape with typical dimensions of $8 \times 1 \times 0.5$ mm³ to which voltage and current taps were made using thin silver-plated copper wires and silver epoxy. The temperature dependences of the upper critical field, H_{c2}, and of the irreversibility field, H_{Irr}, were evaluated with different criteria from 99% R_N to 1% R_N, with R_N being the normal state resistance (99% and 90% R_N are the most used criteria for H_{c2}, whereas 10% and 1% are the most common criteria for H_{Irr}). In the following, the $\mu_0 H_{c2,99}$ notation refers, for instance, to H_{c2} estimated at 99% R_N. Nb₃Sn data were fitted using the reduced WHH equation, where both the paramagnetic limitation parameter (α) and a spin-orbit scattering parameter (λ_{so}) are set to 0. So, we used the follow eq.:

$$\ln \frac{1}{t} = \psi \left(\frac{1}{2} + \frac{\bar{h}}{2t} \right) - \psi \left(\frac{1}{2} \right) \tag{1}$$

where, $t = \frac{T}{T_c}$, $\bar{h} = \frac{4H_{c2}(T)}{\pi^2 T_c |\frac{dH_{c2}}{dT}|_{T_c}}$ and ψ is the digamma function.

There are two fit parameters T_c and H_{c2} (0), with the latter being related to the H_{c2} slope by the relation (2) below. Similarly to [16], [17], the Werthamer-Helfand-Hohenberg (WHH) fits were made from data taken from 2–16 T, which was then used to

determine the zero-temperature H_{c2} and H_{Irr} values. The $H_{c2,99}$ slopes listed in Table I were back calculated using the relation:

$$H_{c2}(0) = 0.693 \, T_c \left. \left| \frac{dH_{c2}}{dT} \right| \right|_{T_c}. \tag{2}$$

The (Nb2Hf)25Sn-HT2 sample had a mild resistance offset of about 13.5 μΩ, comparable to the instrument sensitivity, when measured on the QD rotator in the 16 T PPMS, but no offset was detected when the same sample was remeasured in the 9 T PPMS. Concluding that the offset was caused by the experimental setup, we have subtracted it.

III. RESULTS

As listed in Table I, we fabricated one binary sample, Nb25Sn-HT1, three ternary samples, (Nb2Hf)25Sn-HT2, (Nb1Hf)25Sn-HT3, and (Nb2Hf)25Sn-HT3, and a quaternary sample (Nb4Ta1Hf)25Sn-HT4. The ternary sample, denoted as (Nb1Hf)25Sn, is made of 75 at.% niobium alloy and 25 at.% Sn. Within the niobium alloy, the composition is 99 at.% pure niobium (Nb) and 1 at.% hafnium (Hf) and so on.

Fig. 1 shows the superconducting transitions of all the fabricated bulk samples. Sharp transitions were observed for Nb25Sn-HT1, (Nb2Hf)25Sn-HT2, and (Nb1Hf)25Sn-HT3.

Fig. 2 shows SEM images of two bulk samples. Fig. 2(a) and (b) compare the backscattered-electron (BSE) image of binary Nb25Sn-HT1 and (Nb2Hf)25Sn-HT2. The binary Nb25Sn-HT1 was found to be single-phase with an A15 Sn content of about 25.3%. The dark regions in both images are porosity, while the white-contrast spots in Fig. 2(b) are unreacted Hf particles. EDS revealed that the amount of Hf in the A15 of all the Hf-doped samples is lower than the nominal. The missing Hf appears to be distributed as Hf-rich particles (most likely unreacted Hf) scattered throughout the sample but most visible on the interior surfaces of pores (Fig. 2(c)). SEM-EDS measurements indicated oxygen contents consistent with HfO₂ for large (1–3 μm diameter) Hf-rich phases in and adjacent to the voids. It was, however,
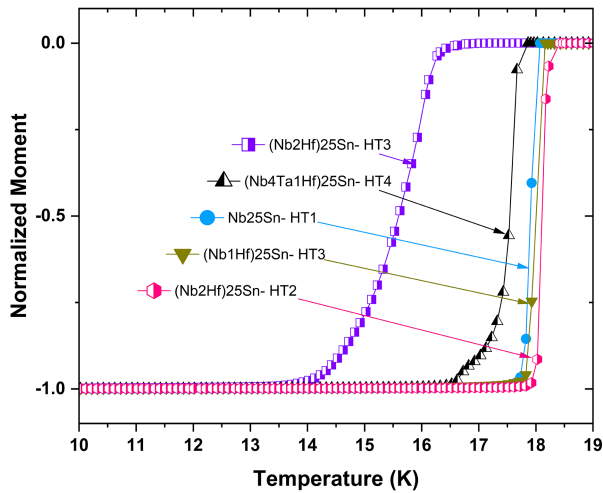
Fig. 1.   Normalized moment versus temperature after zero field cooling to 5 K and then applying 1 mT while warming.

not possible to perform EDS analysis on the smaller particles (which may be relevant for pinning), especially for the particles found in the porous region, because they are too small. Much smaller particles will require additional analysis by TEM.

Fig. 3 shows the resistance versus temperature plot at different fields up to 16 T for the (Nb2Hf)25Sn-HT2 sample. At low fields, the transitions are very sharp, but some transition broadening was observed at higher fields.

Fig. 4 reports a comparison of the temperature dependences of $H_{c2,99}$ and $H_{c2,90}$, including the WHH fits and the zero-temperature H_{c2} extrapolations (also summarized in Table I). We observe that all samples have a $H_{c2,99}$ exceeding 33 T.

Fig. 5 shows the temperature dependence of H_{c2} and H_{Irr} with the WHH fits and 0 K extrapolations at different resistive criteria for the best sample (Nb2Hf)25Sn-HT2. The unusually high extrapolated $\mu_0 H_{c2,99}(0\,K)$ value of 39.2 T and $\mu_0 H_{Irr,1}(0\,K)$ of 30.0 T were observed on this sample, making them the highest H_{c2} and H_{Irr} values ever reported for Nb$_3$Sn in literature. In this case, the $H_{c2,99}$ slope was evaluated as 3.15 T/K.

Differently from the other samples, (Nb1Hf)25Sn-HT3 and (Nb2Hf)25Sn-HT3 were directly heated to 1600 °C/60 h without the 650 °C/16 h pre-annealing step (which was reported to reduce the number of voids [18], [19]). (Nb1Hf)25Sn-HT3 also has a high extrapolated $\mu_0 H_{c2,99}(0\,K)$ of 38.2 T with a slope of 3.11 T/K. EDS revealed 25.2 at.% Sn and 0.40–0.55 at.% Hf in the A15. After the heat treatment, the tube of the (Nb2Hf)25Sn-HT3 sample was found to be cracked with evidence of some Sn leak. The resistivity at 20 K for this sample was the highest, and it was relatively Sn poor (∼24 at.% Sn in A15) and it also had the lowest T_c among all five samples. This sample had the lowest $\mu_0 H_{c2,99}$ (0 K) of 33.1 T.

IV. DISCUSSION

In this work, we have fabricated and characterized bulk Nb$_3$Sn samples with a goal of studying how H_{c2} varies by alloying. To our surprise, we found much broader and higher transitions

than we expected, especially after the recent wide-ranging study of Paudel et al. [16], [17] of H_{c2} using similar arc-melted Nb alloys then reacted to A15 with Cu and Sn powder mixtures. To exemplify our surprise, we can compare our extrapolated $\mu_0 H_{c2,99}(0\,K)$ for binary Nb25Sn-HT1 of 34.6 T with most earlier literature results that generally lie in the 25–31 T range [19], [20], [21]. The only other remotely comparable high value for a binary sample was the 35.7 T $H_{c2}(0)$ reported by Cooley et al. [22] on a heavily ball-milled Nb$_3$Sn powder with heavy disorder that easily annealed away at 750 °C when trying to sinter the powder particles together.

Regarding (Nb2Hf)25Sn, the unusually high $H_{c2,99}(0\,K)$ of 39.2 T is well above the 29.7 T of the property measurement system (PIT) wire [23], 30.8 T of the TaHf-doped wire extrapolated in [24], and above the measured $H_{c2,99}(4.2\,K)$ values obtained in TaHf- and TaZr-doped wires [25] [26], which remain below 30 T. Clearly, our sample is inhomogeneous with a 99%-1% H_{c2}–H_{Irr} breadth of 9 T at 0 K, but both the highest and lowest portions of the transition reach values unseen before. Their unusually high extrapolated H_{c2} values are certainly favored by their high T_c values and their high $H_{c2}(T)$ slopes near T_c up to 3.15 T/K at 99% R_N, leading to the very high $H_{c2}(0)$. To make a further check, we remeasured this same sample in our 9 T PPMS using its resistivity puck rather than the rotator sample holder of the 16 T-PPMS. Using a 2–9 T range for the WHH fit, we obtained a very similar extrapolated $H_{c2,99}$ of about 39 T, confirming the exceptional high result. From the standardless EDS analysis, it was confirmed that the sample had a relatively high Sn content, ∼26.3 at.% Sn, which is unusual compared to any wire, and 0.40–0.50 at.% Hf in the A15.

(Nb4Ta1Hf)25Sn-HT4 is also particularly interesting because in the literature there are now data on many samples with similar doping but reacted below 750 °C. For such wire samples (which are all made in the presence of Cu), $H_{c2}(0)$, though enhanced by about 1 T with respect to similar Hf-free samples, does not exceed 31 T [7], [17], [24], [25], [26]. However, the WHH extrapolated $\mu_0 H_{c2,99}(0\,K)$ of our Cu-free, 1600 °C reacted sample was found to be 36.8 T with a H_{c2} slope of 2.98 T/K. The inhomogeneity of this sample can be seen from the T_c plot shown in Fig. 1, but the predicted 1–99% transition breadth at 0 K was about 8.6 T, similar to the others. The 99% value is high but 90% and 50% are much closer to what expected. Excluding the cracked (Nb2Hf)25Sn-HT3 sample, a general trend of an increase in H_{c2} with an increase in $H_{c2}(T)$ slope and resistivity was observed in these samples, as is seen in Table I.

We initially suspected that these unusually high H_{c2} values might be due to external surface artifacts caused by faster cooling of outer sample regions, which might have retained a higher disorder level than the fully annealed interior regions. However, the pieces for resistivity measurements were taken mostly from the center of the sample. It made no difference whether the sample was tested with or without removing the outer edges. So, we are forced to conclude that these high H_{c2} values are indeed characteristic of our bulk samples.

At this point, we must emphasize that there are differences between these samples and any wires. Wires are always made with Cu present so as to suppress the direct reaction of Nb and Sn
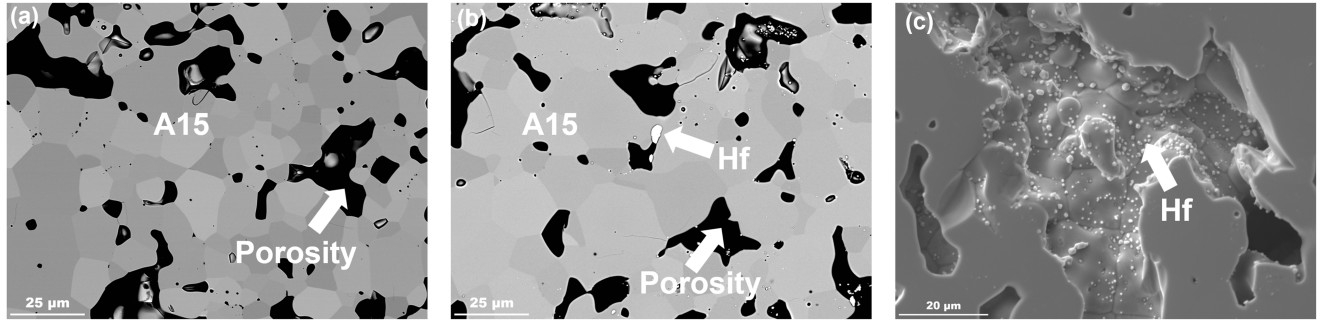
Fig. 2. BSE images of (a) Nb25Sn-HT1 (b) (Nb2Hf)25Sn-HT2. The dark regions represent porosity. (c) Secondary electron image of (Nb2Hf)25Sn-HT2. The "white" particles are the residues of the originally much larger unreacted Hf powder particles.
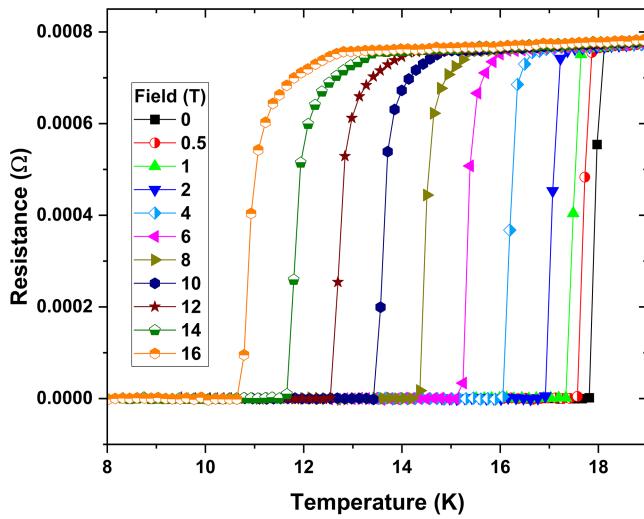

Fig. 3. Transport characterization of (Nb2Hf)25Sn-HT2 at various fields up to 16 T. Resistive offsets were subtracted as described in the text.

Fig. 4. Upper critical field (H_{c2}) versus temperature of all the samples determined using (a) 99% R_N and (b) 90% R_N criteria with WHH fits and the 0 K extrapolations of H_{c2}.

to form $NbSn_2$ and Nb_6Sn_5. These are certainly to be expected in our bulks but they both disappear above 930 °C, allowing full reaction to the only stable phase at 1600 °C, that is Nb_3Sn, which is indeed stable at the stoichiometric composition. Although we rule out external surface artifacts as being the source of the enhanced H_{c2}, the next logical hypothesis to consider is the grain boundary network. Grain boundaries form an internal network that is fully connected and capable of being revealed by our resistivity measurements. A plausible, but so far experimentally unconfirmed interpretation is that grain boundary disorder in Cu-free grain boundaries is enhancing H_{c2}. This grain boundary disorder should affect binary, ternary, or quaternary alloys similarly. Cu segregation to A15 grain boundaries is well supported by many experiments [27], [28], [29]. Since it does not enter the A15 lattice, it is likely to depress the superconducting properties, while Ta and Hf actually enhance them. The principal driver for high H_{c2} is in fact disorder, which reflects itself directly in the H_{c2} slope proportional to $\rho_n T_c$. The enhanced WHH $H_{c2}(0)$ values reported here come directly from the enhanced measured resistivities. The top part of the resistive transitions, measured
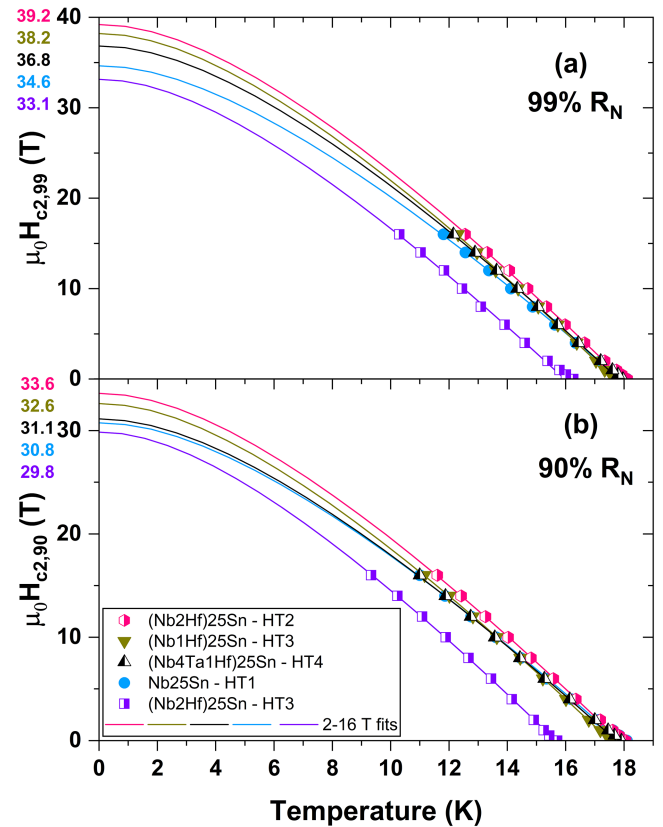
between 90 and 99% of R_N, could represent a minority residual grain boundary superconducting path that is scientifically interesting but impossible to make practical use of.

One final point to note is that Nb_3Sn is a strongly coupled superconductor with a modified BCS Pauli limit H_p. The appropriate relation given by Orlando et al. [30] shows that H_p is enhanced by a factor $\eta_{H_c}(1 + \lambda_{ep})^{\frac{1}{2}}$ with respect to the weakly-coupled case. The λ_{ep} value for binary Nb_3Sn being 1.8 even these unexpectedly high H_{c2} values lie below the Pauli limit.
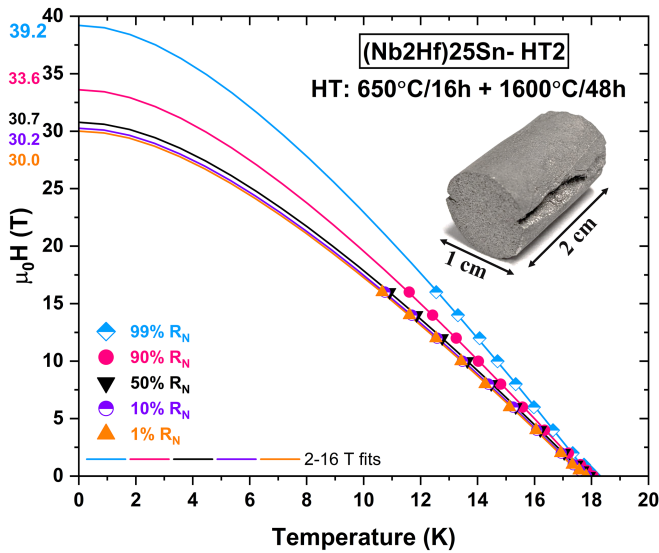
Fig. 5. Upper critical field (H_{c2}) and irreversibility field (H_{Irr}) versus temperature of (Nb2Hf)25Sn-HT2 determined at different resistive criteria with data fitted using the WHH model. The inset shows a picture of the bulk sample before cutting.

Although the recent PhD work of Paudel [16], [17] concludes that the WHH model works well for all Nb$_3$Sn samples and that evaluation up to 16 T is enough to accurately determine $\mu_0 H_{c2}(0\,\mathrm{K})$ eliminating the need to measure at higher fields, we will measure these samples in the 35 T magnet at the NHMFL because these high values demand an explicit verification.

V. Conclusion

Summarizing, all the samples with the highest H_{c2} have a Sn content above 25 at.% and less than 0.6 at.% Hf in the A15 grains. Although our alloyed bulk Nb$_3$Sn samples appear chemically inhomogeneous, they clearly have minority traces of extremely high H_{c2} values never seen before. We plan to thoroughly investigate the origin of these high H_{c2} values, which nearly reach 40 T, because the result is so unexpected. We suspect, but have not yet verified, grain boundary disorder, which is strong even in the binary and also enhanced by doping elements. Also, we do not yet suggest that the results can be translated into wires because all the heat treatments are done at 1600 °C or above and in the absence of Cu, two conditions that are unsuitable for wire manufacture. Our results finally drive home that Nb$_3$Sn, the original high-field superconductor [31] is still not fully understood!

References

[1] A. Ballarino et al., "The CERN FCC conductor development program: A worldwide effort for the future generation of high-field magnets," *IEEE Trans. Appl. Supercond.*, vol. 29, no. 5, Aug. 2019, Art. no. 6001709.

[2] D. Schoerling et al., "The 16 T dipole development program for FCC and HE-LHC," *IEEE Trans. Appl. Supercond.*, vol. 29, no. 5, Aug. 2019, Art. no. 4003109, doi: 10.1109/TASC.2019.2900556.

[3] A. Abada et al., "FCC-HH: The hadron collider," *Eur. Phys. J. Spec. Top.*, vol. 228, pp. 755–1107, 2019, doi: 10.1140/epjst/e2019-900087-0.

[4] M. Benedikt, A. Blondel, P. Janot, M. Mangano, and F. Zimmermann, "Future circular colliders succeeding the LHC," *Nature Phys.*, vol. 16, pp. 402–407, 2020, doi: 10.1038/s41567-020-0856-2.

[5] A. V. Zlobin et al., "Development and first test of the 15 T Nb$_3$Sn dipole demonstrator MDPCT1," *IEEE Trans. Appl. Supercond.*, vol. 30, no. 4, Jun. 2020, Art. no. 4000805, doi: 10.1109/TASC.2020.2967686.

[6] X. Xu, "A review and prospects for Nb$_3$Sn superconductor development," *Supercond. Sci. Technol.*, vol. 30, no. 9, Aug. 2017, Art. no. 093001, doi: 10.1088/1361-6668/aa7976.

[7] S. Balachandran et al., "Beneficial influence of Hf and Zr additions to Nb4at%Ta on the vortex pinning of Nb$_3$Sn with and without an O source," *Supercond. Sci. Technol.*, vol. 32, no. 4, Feb. 2019, Art. no. 044006, doi: 10.1088/1361-6668/aaff02.

[8] R. Akihama, K. Yasukochi, and T. Ogasawara, "The effect of ternary additions to Nb$_3$Sn on the upper critical field at 4.2K," *IEEE Trans. Magn.*, vol. 13, no. 1, pp. 803–806, Jan. 1977, doi: 10.1109/TMAG.1977.1059372.

[9] M. Suenaga et al., "Superconducting critical temperatures, critical magnetic fields, lattice parameters, and chemical compositions of 'bulk' pure and alloyed Nb$_3$Sn produced by the bronze process," *J. Appl. Phys.*, vol. 59, no. 3, Feb. 1986, pp. 840–853, doi: 10.1063/1.336607.

[10] R. Flükiger et al., "Microstructure, composition and critical current density of superconducting Nb$_3$Sn wires," *Cryogenics*, vol. 48, no. 7, pp. 293–307, 2008, doi: 10.1016/j.cryogenics.2008.05.005.

[11] D. Dew-Hughes, "Effect of third element additions on the properties of bronze processed Nb$_3$Sn," *IEEE Trans. Magn.*, vol. 13, no. 1, pp. 651–654, Jan. 1977.

[12] T. Takeuchi, T. Asano, Y. Iijima, and K. Tachikawa, "Effects of the IVa element addition on the composite-processed superconducting Nb$_3$Sn," *Cryogenics*, vol. 21, pp. 585–590, 1981.

[13] W. Goldacker and R. Flükiger, "Phase transitions and superconducting properties of binary and Ti, Ta, Ga and H alloyed Nb$_3$Sn," *Phys. B+C (Amsterdam)*, vol. 135, pp. 359–363, 1985.

[14] R. Bormann, D.-Y. Yu, R. Hammond, T. Geballe, S. Foner, and E. McNiff, "Origin of the B$_{c2}$ enhancement in ternary Nb-Sn phases," *IEEE Trans. Magn.*, vol. TMAG-21, no. 2, pp. 1140–1143, Mar. 1985.

[15] H. Sekine, T. Takeuchi, and K. Tachikawa, "Studies on the composite processed Nb-Hf/Cu-Sn-Ga high-field superconductors," *IEEE Trans. Magn.*, vol. 17, no. 1, pp. 383–386, Jan. 1981.

[16] N. Paudel, "Alloying effects on the upper critical field of Nb$_3$Sn superconductor," Ph.D. dissertation, Dept. Phys., Florida State Univ., 2023. [Online]. Avaialble: https://purl.lib.fsu.edu/diginole/Paudel_fsu_0071E_18400

[17] N. Paudel et al., "Influence of Nb alloying on Nb recrystallization and the upper critical field of Nb$_3$Sn," *Phys. Rev. Mater.*, vol. 8, Aug. 2024, Art. no. 084801, doi: 10.1103/PhysRevMaterials.8.084801.

[18] S. Cogan, D. S. Holmes, and R. M. Rose, "On the elimination of Kirkendall voids in superconducting composites," *Appl. Phys. Lett.*, vol. 35, no. 7, pp. 557–559, 1979, doi: 10.1063/1.91178.

[19] J. Zhou et al., "Evidence that the upper critical field of Nb$_3$Sn is independent of whether it is cubic or tetragonal," *Appl. Phys. Lett.*, vol. 99, no. 12, Sep. 2011, Art. no. 122507, doi: 10.1063/1.3643055.

[20] S. Foner and E. J. McNiff, "Upper critical fields of cubic and tetragonal single crystal and polycrystalline Nb$_3$Sn in DC fields to 30 tesla," *Solid State Commun.*, vol. 39, no. 9, pp. 959–964, 1981, doi: 10.1016/0038-1098(81)90065-X.

[21] M. C. Jewell, "The upper critical field of stoichiometric and off-stoichiometric bulk, binary Nb$_3$Sn," *AIP Conf. Proc.*, vol. 711, pp. 474–484, 2004, doi: 10.1063/1.1774604.27.

[22] L. D. Cooley, Y. F. Hu, and A. R. Moodenbaugh, "Enhancement of the upper critical field of Nb$_3$Sn utilizing disorder introduced by ball milling the elements," *Appl. Phys. Lett.*, vol. 88, no. 14, Apr. 2006, Art. no. 142506, doi: 10.1063/1.2193047.

[23] A. Godeke, M. C. Jewell, C. M. Fischer, A. A. Squitieri, P. J. Lee, and D. C. Larbalestier, "The upper critical field of filamentary Nb$_3$Sn conductors," *J. Appl. Phys.*, vol. 97, no. 9, May 2005, Art. no. 093909, doi: 10.1063/1.1890447.

[24] C. Tarantini et al., "Origin of the enhanced Nb_3Sn performance by combined Hf and Ta doping," *Sci. Rep.*, vol. 11, 2021, Art. no. 17845, doi: 1038/s41598-021-97353-w.

[25] G. Bovone et al., "Effects of the oxygen source configuration on the superconducting properties of internally-oxidized internal-Sn Nb_3Sn wires," *Supercond. Sci. Technol.*, vol. 36, no. 9, Aug. 2023, Art. no. 095018, doi: 10.1088/1361-6668/aced25.

[26] F. Buta et al., "Very high upper critical fields and enhanced critical current densities in Nb_3Sn superconductors based on Nb–Ta–Zr alloys and internal oxidation," *J. Phys.: Mater.*, vol. 4, no. 2, Mar. 2021, Art. no. 025003, doi: 10.1088/2515-7639/abe662.

[27] M. Suenaga and W. Jansen, "Chemical compositions at and near the grain boundaries in bronze-processed superconducting Nb_3Sn," *Appl. Phys. Lett.*, vol. 43, no. 8, pp. 791–793, Oct. 1983, doi: 10.1063/1.94457.

[28] D. Rodrigues, C. L. H. Thieme, D. G. Pinatti, and S. Foner, "Grain boundary compositions, transport and flux pinning of multifilamentary Nb_3Sn wires," *IEEE Trans. Appl. Supercond.*, vol. 5, no. 2, pp. 1607–1610, Jun. 1995, doi: 10.1109/77.402881.

[29] M. Sandim et al., "Grain boundary segregation in a bronze-route Nb_3Sn superconducting wire studied by atom probe tomography," *Supercond. Sci. Technol.*, vol. 26, no. 5, 2013, Art. no. 055008, doi: 10.1088/0953-2048/26/5/055008.

[30] T. P. Orlando, E. J. McNiff, S. Foner, and M. R. Beasley, "Critical fields, Pauli paramagnetic limiting, and material parameters of Nb_3Sn and V_3Si," *Phys. Rev. B*, vol. 19, 1979, Art. no. 4545.

[31] J. E. Kunzler et al., "Superconductivity in Nb_3Sn at high current density in a magnetic field of 88 kgauss," *Phys. Rev. Lett.*, vol. 6, 1961, Art. no. 89, doi: 10.1103/PhysRevLett.6.89.